Enhanced catalytic activity of potassium-doped graphitic carbon nitride induced by lower valence position

Mo Zhang, Xiaojuan Bai, Di Liu, Jun Wang, Yongfa Zhu *

Department of Chemistry, Beijing Key Laboratory for Analytical Methods and Instrumentation, Tsinghua University, Beijing 100084, China

ARTICLE INFO

ABSTRACT

The potassium doped graphitic carbon nitride (K-C$_3$N$_4$) photocatalysts were prepared via thermal polymerization of dicyandiamide and KI in atmosphere. The valence band (VB) position of g-C$_3$N$_4$ was decreased via potassium doping, resulting in enhanced separation and immigration of photogenerated carriers under visible light. The optimum K-C$_3$N$_4$ exhibited obviously enhanced photocatalytic activities for phenol and MB degradation, which were about 3.3 and 5.8 times as high as those of bulk g-C$_3$N$_4$, respectively. The photocatalytic activity of K-C$_3$N$_4$ decreased with excessive KI mass fraction in the precursor due to the incomplete polymerization of g-C$_3$N$_4$.

© 2014 Published by Elsevier B.V.

1. Introduction

Photocatalysis is regarded as a promising technique to deal with the problems of resources and environment [1–5]. Graphitic carbon nitride (g-C$_3$N$_4$) has been widely applied in water decomposition, oxygen reduction, organic photosynthesis and environmental remediation, due to its visible light activity and chemical stability [6–8]. However, its photocatalytic degradation ability of organic pollutants, especially benzene-based organics, is seriously limited by its low catalytic activity and ring opening ability due to the high valence band (VB) position [9]. In addition, the fast charge recombination is another drawback to limit the photocatalytic activity [10,11]. Hence, the development of g-C$_3$N$_4$ with lower VB position, considerable catalytic activity and enhanced charge separation and immigration has become an urgent necessity.

Among all the strategies to enhance the activity of photocatalysts, doping is one of the most intensively researched methods [12–16]. Nonmetal doping can increase the visible light absorption, modify the carrier mobility of catalysts and modulate the electronic structure of catalysts [11,17]. Phosphorus doped g-C$_3$N$_4$ can provided a much better electric (dark) conductivity and an improved photocurrent [11]. Sulfur doped graphitic C$_3$N$_4$ (C$_3$N$_{4-x}$S$_x$) is reported to display increased valence bandwidth and elevated conduction band minimum [18]. However, the valence

position of the catalysts is difficult to decrease by nonmetal, which may limit their application in organic pollutants degradation. Alkali doping can modulate the electronic structure of materials, which may change the performance of the catalysts [19,20]. In consideration of the drawbacks of fast charge recombination, high VB position, low catalytic activity and ring opening ability of g-C$_3$N$_4$, alkali doping may modulate the electronic structure and promote the catalytic activity of g-C$_3$N$_4$. C$_3$N$_4$-based intercalated compound with alkali metals can induce the non-uniform spatial charge distribution and enhance the separation efficiency of photogenerated carriers [21]. In addition, potassium-modified g-C$_3$N$_4$ can effectively reduce the recombination rate of photogenerated electron–hole pairs and shows high photocatalytic for hydrogen evolution [22]. Although alkali metals doped g-C$_3$N$_4$ has been researched, g-C$_3$N$_4$ with modulate electronic structure and catalytic activity for organic pollutants degradation is rarely realized by alkali doping.

Herein, potassium is chosen as dopant into g-C$_3$N$_4$ to demonstrate the conception above. The valence band position of g-C$_3$N$_4$ shifted to a lower energy position via potassium doping. The photocatalytic activities of K-C$_3$N$_4$ were about 3.3 and 5.8 times as high as those of bulk g-C$_3$N$_4$ for phenol and MB degradation, which can ascribe to the decreased valence position and the enhanced separation and immigration of photogenerated carriers under visible light. This work provides a simple and low-cost method to synthesize the doping catalyst, which shed light on great potentials for application in treatment of environmental pollution.

* Corresponding author. Tel.: +86 10 6278 3586; fax: +86 10 6278 7601.
E-mail address: zhuyf@mail.tsinghua.edu.cn (Y. Zhu).

2. Experimental

2.1. Synthesis of photocatalyst

Dicyandiamide was purchased from Sinopharm Chemical Reagent Corp, PR China. All other reagents used in this research were analytically pure and used without further purification.

The K-C$_3$N$_4$ photocatalysts were prepared by thermal polymerization of dicyandiamide and KI in atmosphere. The typical preparation of K-g-C$_3$N$_4$ photocatalysts was as follows: 5 g of dicyandiamide and KI was put in a Muffle Furnace and heated to 550 °C for 4 h to complete the reaction. The yellow products were washed with nitric acid (0.1 mol L^{-1}) and deionized water to remove the residue adsorbed on the surface of g-C$_3$N$_4$. Then the pure products were dried at 80 °C for 12 h.

2.2. Characterizations

The morphologies and structures of the samples were examined with HITACHI HT7700 transmission electron microscopy (TEM) operated at an accelerating voltage of 100 kV. UV–vis diffuse reflectance spectroscopy (DRS) was carried out on a Hitachi U-3010 UV-vis Spectrophotometer using BaSO$_4$ as the reference. The crystallinity of the as-prepared sample was characterized by X-ray diffraction (XRD) on Bruker D8-advance diffractometer using Cu-Kα radiation (λ = 1.5418 Å). The photocurrents were measured on an electrochemical system (CHI 660D, China). Raman spectra were obtained by using a HORIBA JY HR800 confocal microscope Raman spectrometer employing an Ar-ion laser (633 nm). A 50× telephoto Olympus objective lens was used to focus the laser on the samples. All spectra were calibrated with respect to silicon wafer at 520.7 cm^{-1}. Fourier transformed infrared (FTIR) spectra were recorded on a Bruker VERTEX 700 Spectrometer. Photoluminescence spectra (PL) of the samples were obtained at room temperature using a HORIBA Aqualog Fluorescence Spectrometer.

2.3. Photocatalytic experiments

The photocatalytic activities were evaluated by the decomposition of phenol under visible light irradiation (λ > 420 nm) and simulated sunlight irradiation. Visible irradiation was obtained from a 500 W Xe lamp (Institute for Electric Light Sources, Beijing) with a 420 nm cutoff filter, and the average visible light intensity was 35 mW cm^{-2}. For the photocatalytic experiments, 25 mg of photocatalyst was totally dispersed in an aqueous solution of phenol (50 mL, 5 ppm). Before irradiation, the suspensions were magnetically stirred in the dark for 2 h to get absorption–desorption equilibrium between the photocatalyst and phenol. At certain time intervals, 3 mL aliquots were sampled and centrifuged to remove the particles. The concentration of phenol was analyzed by chromatographic experiments with HPLC–UV/vis system.

2.4. Analyses of the degradation intermediates for phenol

The chromatographic experiments with HPLC–UV/vis system were carried out using an ultraviolet absorbance detector (K 2501) operated at 275 nm phenol coupled to a Venusil XBP-C18 (Agela Technologies Inc.) column. Before the analysis, the samples were filtered through millipore discs of 0.45 μm to protect the chromatographic column. The mobile phase used for eluting phenol and its degradation intermediates from the HPLC columns consisted of methanol and water (60:40, v/v) at a flow rate of 1 mL min^{-1}.

Table 1
The concentrations of elements for different materials determined by XRF.

Materials	N	C	O	K	I
Pure C$_3$N$_4$	68.89%	29.05%	1.41%	0	0
10%-K-g-C$_3$N$_4$	65.08%	27.61%	1.93%	4.58%	0.72%
16%-K-g-C$_3$N$_4$	64.37%	27.95%	2.12%	4.93%	0.59%
22%-K-g-C$_3$N$_4$	63.69%	27.81%	2.61%	5.47%	0.35%
27%-K-g-C$_3$N$_4$	62.81%	28.31%	2.85%	5.66%	0.30%
30%-K-g-C$_3$N$_4$	63.69%	28.14%	3.28%	4.58%	0.20%

2.5. Photoelectrochemical measurements

To investigate the transition of photogenerated electrons of K-g-C$_3$N$_4$, a standard three-electrode cell with a working electrode (as-prepared photocatalyst, a platinum wire as counter electrode, and a saturated calomel electrode (SCE) as reference electrode were used in the photoelectric studies. 0.1 M Na$_2$SO$_4$ was used as the electrolyte solution. Potentials are given with reference to the SCE. The photoresponses of the photocatalysts as light on and off were measured at 0.0 V. The working electrodes were prepared as follows: 5 mg of the as-prepared photocatalyst was suspended in 1 mL water to produce slurry, which was then dip-coated onto a 2 cm × 4 cm indium tin oxide (ITO) glass electrode. Electrodes were exposed to air atmosphere for 12 h to eliminate water and subsequently calcined at 200 °C for 5 h.

3. Results and discussions

The concentrations of elements for different materials are explored by X-ray fluorescence spectroscopy (XRF). As shown in Table 1, the potassium concentration increases with the increasing KI content in the precursor with mass fraction of KI from 0% to 27%. The decreased potassium concentration of 30%-K-C$_3$N$_4$ may be ascribed to the incomplete polymerization of dicyandiamide with excessive KI. When the KI mass fraction is cross the threshold of 27%, the contact area between K and dicyandiamide is decreased and the most of the KI tends to thermal decompose instead of react with dicyandiamide. The chemical states of potassium were revealed by measuring K 2p levels using XPS. The K2p peaks of 22%-K-C$_3$N$_4$ are explored by peak separation (Fig. 1). The K2p3/2 and K2p1/2 peaks for 22%-K-C$_3$N$_4$ are discovered at 292.8 and 295.3 eV, which are lower than potassium salt [23]. Interestingly, the peak locations of K2p3/2 and K2p1/2 for K-C$_3$N$_4$ are increased with increasing KI content in the precursor (Fig. S1), indicating the existent of covalent bond between K and C$_3$N$_4$.
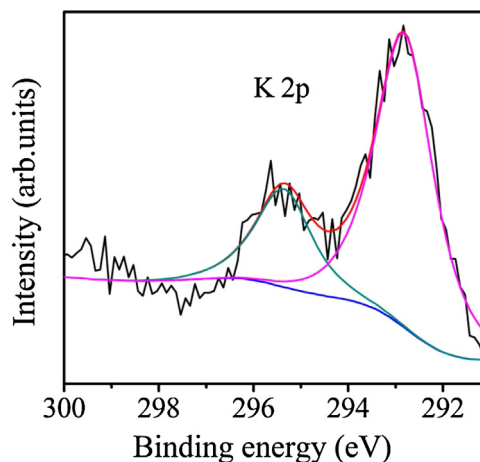

Fig. 1. The K2p XPS spectrum of 22%-K-C$_3$N$_4$.